Full Paper

Synthesis and Biological Evaluation of 10-^{11}C-Dihydrotetrabenazine as a Vesicular Monoamine Transporter 2 Radioligand

Xiaomin Li, Zhengping Chen, Jie Tang, Chunyi Liu, Pei Zou, Hongbo Huang, Cheng Tan, and Huixin Yu

Key Laboratory of Nuclear Medicine, Ministry of Health, Jiangsu Key Laboratory of Molecular Nuclear Medicine, Jiangsu Institute of Nuclear Medicine, Wuxi, P. R. China

In this study, we synthesized a new carbon-11-labeled radiotracer, 10-^{11}C-dihydrotetrabenazine (10-^{11}C-DTBZ), and evaluated its potential as a vesicular monoamine transporter 2 (VMAT2) radioligand. The radiolabeled precursor 10-*O*-desmethyl-dihydrotetrabenazine (10-*O*-desmethyl-DTBZ) was prepared with a six-step reaction using 3-methoxy-4-benzyloxybenzaldehyde as starting material. 10-^{11}C-DTBZ was synthesized by heating 1.0 mg of 10-hydroxy precursor and ^{11}C-methyl iodide in the presence of 0.3 mL of dimethyl sulfoxide and 4.0 μL of 3 N KOH at room temperature for 3 min. After purification by solid phase extraction using an alumina Sep-Pak cartridge, the final 10-^{11}C-DTBZ product was obtained with a radiochemical purity of >99% and an uncorrected radiochemical yield of 18–26% (end of bombardment (EOB), $n = 6$). The overall synthesis time was approximately 20 min from the EOB to release of the product for quality control. Using small-animal positron emission tomography (microPET), the striatum of normal rats was found to exhibit symmetrical labeling ($ST_R/ST_L = 0.98 \pm 0.05$, $n = 3$) and the highest uptake of radioactivity (striatum/cerebellum, $ST/CB = 2.89 \pm 0.31$ at 30–60 min, $n = 3$). In contrast, rats with 6-hydroxydopamine unilateral lesions yielded asymmetrical striatal images with a higher 10-^{11}C-DTBZ concentration on the unlesioned side ($ST_{unlesioned}/CB = 2.53 \pm 0.18$, at 30–60 min, $n = 3$) compared with the lesioned side ($ST_{lesioned}/CB = 1.26 \pm 0.10$, $n = 3$). These results suggest that 10-^{11}C-DTBZ may represent a promising PET radiotracer for imaging VMAT2.

Keywords: Carbon-11 / Dihydrotetrabenazine / Parkinson's disease / Positron emission tomography / Vesicular monoamine transporter

Received: August 15, 2013; Revised: November 14, 2013; Accepted: November 15, 2013

DOI 10.1002/ardp.201300307

Introduction

In the brain, vesicular monoamine transporter 2 (VMAT2) is localized exclusively in presynaptic monoaminergic terminals and is predominantly expressed in rodent and human monoaminergic neurons of the central nervous system (CNS). Therefore, the imaging of VMAT2 in the brain with positron emission tomography (PET) enables the quantification of neuronal densities, and this technique has been used to diagnose and monitor neurological and psychiatric disorders such as Parkinson's disease (PD), Huntington's disease (HD), Alzheimer's disease (AD), and schizophrenia [1–4].

In the past two decades, a wide variety of radioligands, including tetrabenazine (TBZ) analogs, ketanserin analogs, lobeline analogs, and 3-amine-2-phenylpropene analogs, have been developed for *in vitro* and *in vivo* studies of VMAT2 in both the animal and human brain [5–8]. Among these compounds, analogs of TBZ (Nitoman®) are promising because of their high, selective affinity for VMAT2, high cerebral accumulation, suitable lipophilicity, short-lived pharmacological effects, and low toxicity. Furthermore, these analogs have been synthesized and used for *in vivo* brain imaging of VMAT2 with PET, including [^{11}C]tetrabenazine ([^{11}C]TBZ),

Correspondence: Prof. Zhengping Chen, Key Laboratory of Nuclear Medicine, Ministry of Health, Jiangsu Institute of Nuclear Medicine, No. 20 Qianrong Road, Wuxi 214063, P. R. China.
E-mail: chenzhengping@jsinm.org
Fax: +86 0510 85513113

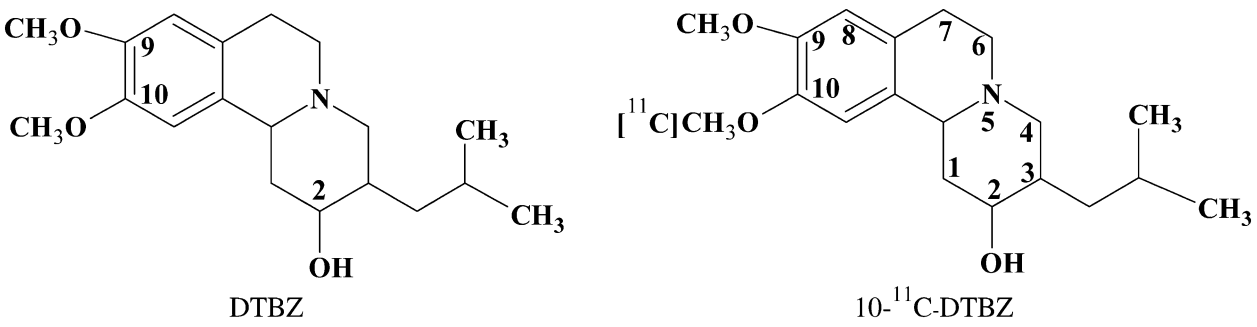

Figure 1. Structures of DTBZ and 10-^{11}C-DTBZ.

9-[^{11}C]dihydrotetrabenazine (9-^{11}C-DTBZ), [^{11}C]methoxytetrabenazine ([^{11}C]MTBZ), and 9-[^{18}F]fluoropropyl-(+)-desmethyldihydrotetrabenazine (9-[^{18}F]FP-(+)-DTBZ) [9–12].

TBZ is a well-characterized antipsychotic drug that has been used clinically for more than five decades. *In vivo*, TBZ is rapidly and extensively metabolized to its reduced form, dihydrotetrabenazine (DTBZ, see Fig. 1). DTBZ has been labeled with ^{3}H on the C-2 hydrogen and successfully used as a selective radioligand in *in vitro* brain homogenate binding studies and in autoradiographic studies [13, 14]. DTBZ has also been labeled with ^{11}C on the 9-*O*-methyl group of the aromatic ring and applied in the diagnosis and monitoring of VMAT2-related disorders such as PD [15, 16].

Continuing the active research in this area, we herein report the synthesis of a novel carbon-11-labeled DTBZ derivative in order to explore the effect of 10-*O*-[^{11}C]methoxyl group on the specific brain uptake and retention, and metabolism.

In this study, 3-isobutyl-9-methoxy-10-[^{11}C]-methoxy-2,3,4,6,7,11*b*-hexahydro-1*H*-pyrido[2,1-*a*]isoquinoline-2-ol (10-^{11}C-DTBZ) (see Fig. 1), labeled on the 10-*O*-methyl position of the aromatic ring, was synthesized and imaged using small-animal PET (microPET) in rats to evaluate its potential as an *in vivo* radioligand for imaging VMAT2.

Results and discussion

Chemistry

The radiolabeled precursor 3-isobutyl-9-methoxy-2,3,4,6,7,11*b*-hexahydro-1*H*-pyrido[2,1-*a*]isoquinoline-2,10-diol (10-*O*-desmethyl-DTBZ) was synthesized in a six-step reaction from the starting material 3-methoxy-4-benzyloxybenzaldehyde. The target compound was identified by IR, ESI-MS, and ^{1}H NMR, and the results agreed well with the expected chemical structure. The general synthetic procedure for 10-*O*-desmethyl-DTBZ is shown in Scheme 1.

The starting compound (**1**) was prepared in good yield (75%) via a Knoevenage reaction of 3-methoxy-4-benzyloxybenzaldehyde, ammonium acetate, and nitromethane in acetic acid under refluxing. Then, compound **1** was reacted further by a

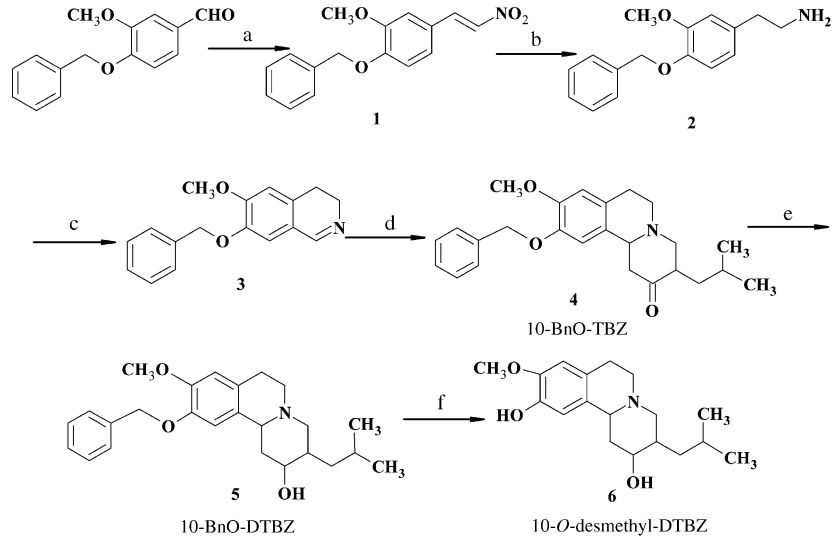

Scheme 1. Synthesis of 10-*O*-desmethyl-DTBZ. Reactions and conditions: (a) CH_3NO_2, NH_4Ac, HAc, 130°C, 2 h; (b) $LiAlH_4$, THF, Et_2O, 60°C, 2 h; (c) HMTA, HAc, TFA, 80°C, 2 h; (d) 3-dimethylaminomethyl-5-methyl-hexan-2-one, TEBAC, H_2O, 90°C, 4 h; (e) $NaBH_4$, EtOH, r.t., 16 h; (f) H_2, Pd/C, EtOH, r.t., 16 h.

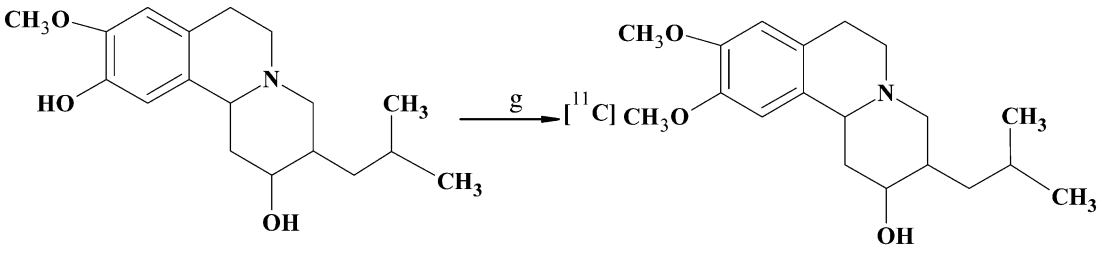

6 10-*O*-desmethyl-DTBZ **7** 10-^{11}C-DTBZ

Scheme 2. Radiochemical synthesis of 10-^{11}C-DTBZ. Reagents and conditions: (g) ^{11}C-CH_3I, DMSO, 3 N KOH, r.t., 3 min.

$LiAlH_4$ reduction reaction to yield compound **2**. Compound **3** was created via the reaction of Bischler–Napieralski in the presence of HMTA. We synthesized 3-dimethylaminomethyl-5-methyl-hexan-2-one using our previously described process [17]. Compound **4** was obtained by Michael addition at 90°C, which was catalyzed using triethylbenzylammonium chloride (TEBAC) in water. The reduction of compound **4** in the presence of $NaBH_4$ yielded compound **5**. Finally, deprotection of the benzyl group of compound **5** via hydrogenolysis using a Pd/C catalyst resulted in target compound **6**.

Radiochemistry

Radiosynthesis from the 10-hydroxy precursor was conducted as shown in Scheme 2. 10-^{11}C-DTBZ was prepared according to the reported procedure with some modifications [18].

A simple, rapid, semi-automated method for the synthesis of 10-^{11}C-DTBZ was developed. $^{11}CO_2$ was produced by a $^{14}N(p,\alpha)^{11}C$ nuclear reaction on a target of nitrogen gas using a HM-7 cyclotron (Sumitomo Heavy Industries, Ltd., Japan). The $^{11}CO_2$ produced was transported to an automated synthesis system of ^{11}C-methyl iodide. 10-^{11}C-DTBZ was synthesized by rapid 10-*O*-[^{11}C]methylation of compound **6** with ^{11}C-methyl iodide as a methylation agent.

After purification by solid-phase extraction using an alumina Sep-Pak cartridge, the final 10-^{11}C-DTBZ product was obtained. The radiochemical yield of 10-^{11}C-DTBZ was 18–26% ($n = 6$) without decay correction at the end of bombardment (EOB). Further optimization of the process may successfully increase the total yield. The overall synthesis time was approximately 20 min from EOB to release of the product for quality control.

Quality control

The identity of 10-^{11}C-DTBZ was confirmed by comparing the retention time of the radioactive product with that of the cold compound, DTBZ, by HPLC. The retention time of 10-^{11}C-DTBZ was 7.8 min, which matched well with that of DTBZ within an admissible error (Fig. 2). The radiochemical purity (RCP) exceeded 99%, and the product was radiochemically stable for at least 1 h. The chemical purity of 10-^{11}C-DTBZ after purification was greater than 95%. The specific radioactivity (SA) was 45 ± 14 GBq/μmoL (end of synthesis, $n = 6$). It is expected that further optimization of the process would raise the value of SA.

MicroPET imaging

10-^{11}C-DTBZ binding to VMAT2 in the brain was demonstrated *in vivo* by performing microPET imaging in normal and 6-hydroxydopamine (6-OHDA) unilaterally lesioned rats.

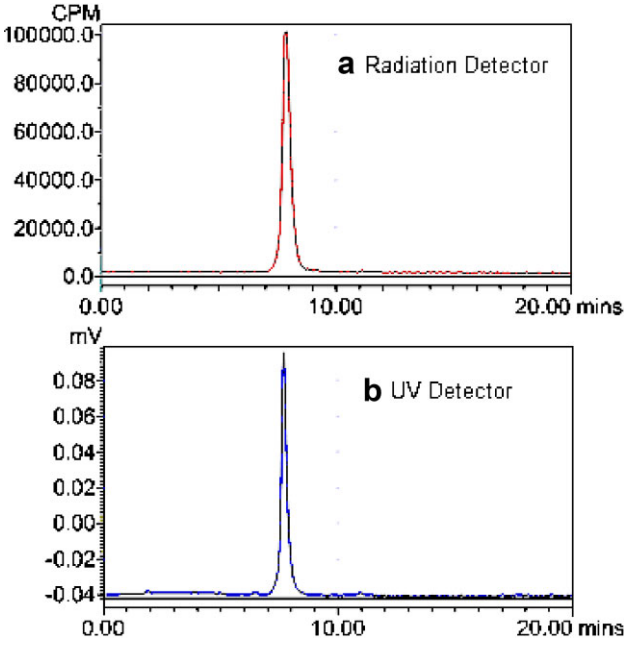

Figure 2. RCP of 10-^{11}C-DTBZ analyzed by HPLC. The chromatograms of purified 10-^{11}C-DTBZ were determined with a radiation detector, and the co-injection of DTBZ with a UV detector was performed under the same HPLC analytical conditions. 10-^{11}C-DTBZ exhibited the same retention time as cold DTBZ.

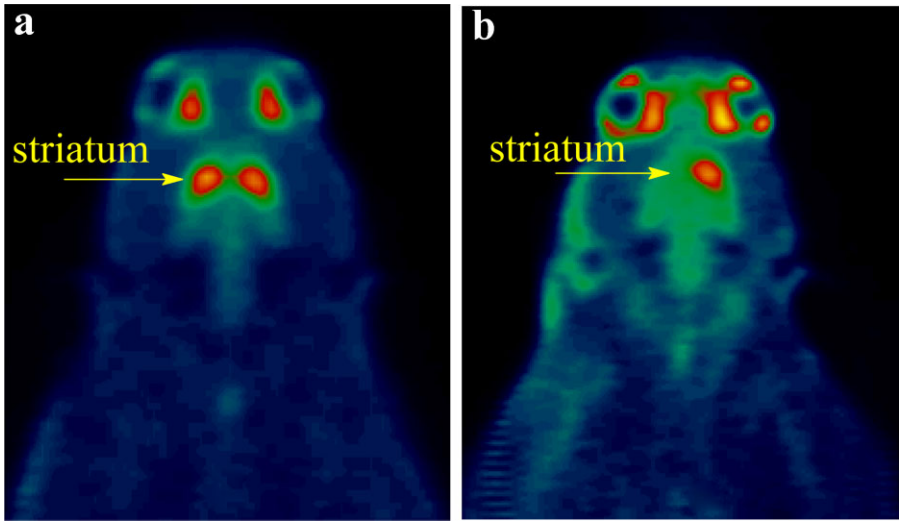

Figure 3. *In vivo* 10-^{11}C-DTBZ microPET studies of normal and 6-OHDA-lesioned PD rats. PET images of 10-^{11}C-DTBZ in the brains of normal (a) and 6-OHDA-lesioned PD (b) rats. PET data were collected using an animal PET scanner with a transaxial resolution of 1.4 mm. Each PET image was generated by the summation of data collected 8–60 min after injection.

Coronal microPET images of normal and unilateral 6-OHDA-lesioned rat brains at 8–60 min after tail vein injection of 10-^{11}C-DTBZ are shown in Fig. 3a and b, respectively.

MicroPET imaging with 10-^{11}C-DTBZ in normal rats produced high-quality images, as shown in Fig. 3a. A high accumulation of radioactivity was observed in the striatum, the site with the highest concentrations of VMAT2. In contrast to the symmetrical uptake of the radioligand in the brains of normal rats, in unilateral 6-OHDA-lesioned rats (see Fig. 3b), the radioactivity of the tracer was localized to the unlesioned side in distinct levels, whereas almost no visible uptake of 10-^{11}C-DTBZ was observed on the lesioned side in microPET images. These *in vivo* microPET results confirmed the affinity of 10-^{11}C-DTBZ to VMAT2.

Figure 4 shows time–radioactivity curves for the striatum and cerebellum following tail vein injection of 10-^{11}C-DTBZ. After the injection of 10-^{11}C-DTBZ, the radioactivity was rapidly taken up by the brain, with the striatum and cerebellum exhibiting maximal activity at ~1 min. The egress of radioactivity from brain regions was also very rapid, with good differentiation of the striatum from the cerebellum visible between 8 and 60 min after injection. In the cerebellum, the time–activity curve showed a peak within 1 min post-injection and then fell off rapidly. In the meanwhile, the striatum exhibited the highest uptake level and good retention of the radioligand. The striatum to cerebellum ratio (ST/CB) of radioactivity reached a maximum value of 2.89 ± 0.31 at 30 min after injection. In the microPET images, the striatum of normal rats exhibited symmetrical labeling ($ST_R/ST_L = 0.98 \pm 0.05$, $n = 3$) and the highest uptake of radioactivity ($ST/CB = 2.89 \pm 0.31$ at 30–60 min, $n = 3$). In contrast, 6-OHDA unilateral lesioned rats yielded asymmetrical striatal images with a higher 10-^{11}C-DTBZ concentration on the unlesioned side ($ST_{unlesioned}/CB = 2.53 \pm 0.18$, at 30–60 min, $n = 3$) compared with the lesioned side ($ST_{lesioned}/CB = 1.26 \pm 0.10$, $n = 3$).

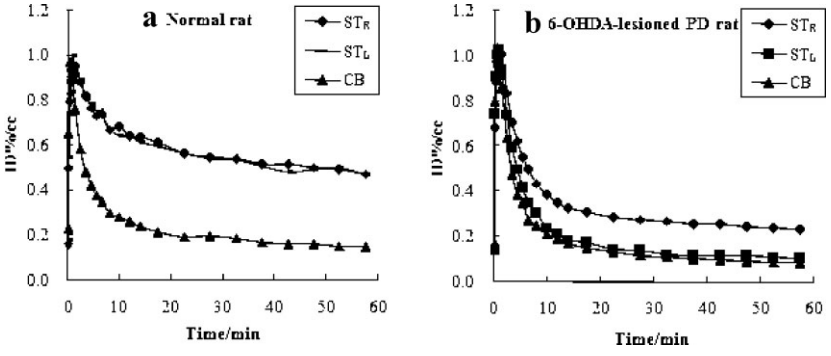

Figure 4. Time–activity curves of 10-^{11}C-DTBZ in the brains of normal and 6-OHDA-lesioned PD rats, expressed as the ID%/cc, for the right striatum (ST_R), left striatum (ST_L), and cerebellum (CB). PET data were collected for 60 min. Regions of interest (ROIs) were identified according to the stereotaxic atlas. The radioactivities in the striatum and cerebellum were plotted against the time post-injection.

These microPET images of rat brains indicated a high level of uptake in the striatal regions rich in VMAT2 but low uptake in the cerebellum. The time–activity curves of 10-^{11}C-DTBZ also revealed high-level accumulation in the striatum, with a low level in the cerebellum of the rat brain. The rapid brain uptake and clearance kinetics of 10-^{11}C-DTBZ were similar to those of many previously reported radioligands, such as ^{11}C-TBZ, ^{11}C-MTBZ, 9-^{11}C-DTBZ, 9-^{11}C-(+)-DTBZ, 9-^{18}F-FE-DTBZ, and 9-^{18}F-FP-DTBZ [19–23]. The striatum-to-cerebellum ratio was maximal (2.89 ± 0.31) at 30 min post-injection, which was higher than that previously reported for ^{11}C-MTBZ (2.7 ± 0.4) [20], 9-^{18}F-FE-DTBZ (2.55) [24], and ^{11}C-TBZ (2.85 ± 0.52) [25] but lower than that for 9-^{11}C-(+)-DTBZ (5.24) [24] and 9-^{18}F-FP-DTBZ (5.08 ± 0.81) [26]. In addition, the uptake of 10-^{11}C-DTBZ was sharply decreased in the striatum in the lesioned side of 6-OHDA unilateral lesioned rats. These results were consistent with many reports of VMAT2 imaging in unilateral 6-OHDA-lesioned rats using 9-^{11}C-(+)-DTBZ, 9-^{18}F-FP-DTBZ, or a variety of radiolabeled VMAT2 ligands [26, 27]. Together, these results suggest that 10-^{11}C-DTBZ may serve as a radiotracer with favorable properties for quantifying brain VAMT2 function with PET. Additional evaluations, such as brain biodistribution studies, blocking experiments, and metabolism profiles are in progress and will be reported in the future.

The tracer used in this study was a racemic mixture of the (+) and (−) enantiomers, and it was previously reported that the *in vitro* binding of (±)-DTBZ was stereospecific, with a high binding affinity ($K_i = 0.97$ nM) only for (+)-DTBZ [28]. Thus, an improved target-to-nontarget ratio (ST/CB) of 10-^{11}C-(+)-DTBZ should be expected, and further studies in the rodent brain with 10-^{11}C-(+)-DTBZ are ongoing.

Conclusions

In this study, we designed, synthesized, and evaluated the biological characteristics of a novel carbon-11-labeled DTBZ derivative, 10-^{11}C-DTBZ. 10-^{11}C-DTBZ was synthesized by rapid 10-*O*-[^{11}C]methylation of desmethyl-DTBZ with ^{11}C-methyl iodide and obtained at a high RCP. *In vivo* microPET studies demonstrated that 10-^{11}C-DTBZ showed high brain uptake and high affinity and specificity for brain VMAT2. Therefore, 10-^{11}C-DTBZ may serve as a probe for the *in vivo* PET imaging of monoaminergic terminal loss associated with neurological disease.

Experimental

All chemicals were commercially obtained and used without further purification unless otherwise noted. Melting points were measured using a Yanaco MP-S3 melting point apparatus (Shimadzu, Japan). Nuclear magnetic resonance (NMR) spectra were recorded on a Bruker AVANCE-III 400 MHz spectrometer (Bruker, Germany), and the chemical shift value was given relative to the internal tetramethylsilane (TMS) standard. Electron spray ion (ESI) mass spectra were determined using a Waters Platform ZMD 4000 LC/MS (Waters, USA). IR data were obtained using a Bruker Tensor 27 FT-IR infrared spectrophotometer (Bruker, Germany). The high-performance liquid chromatography (HPLC) analysis system for characterizing 10-^{11}C-DTBZ consisted of a binary HPLC pump (Waters 1525, USA), a UV detector (Waters 2487, USA), and a flow scintillation analyzer (Radiomatic 610TR, Perkin-Elmer, USA). All Sprague-Dawley rats were supplied by the Shanghai SLAC Laboratory Animal Co., Ltd. (Shanghai, China). The 6-OHDA was purchased from Sigma Co., and the left-sided 6-OHDA-lesioned PD rats were established as previously described [29]. All the animal experiments were carried out in compliance with the relevant national laws associated with the conduct of animal experimentation.

Chemistry

*3-Methoxy-4-benzyloxy-β-nitrostyrene (**1**)*

Nitromethane (10.25 mL, 191 mmol) was added to a solution of 3-methoxy-4-benzyloxybenzaldehyde (20.64 g, 85.3 mmol) and ammonium acetate (6.45 g, 83.77 mmol) in acetic acid (66 mL) at 40°C. The reaction mixture was heated to reflux at 130°C for 2 h and then cooled to room temperature. The crude product was purified by crystallization with ethanol to produce compound **1** (17.9 g, 75%) as a yellow crystal with the following properties: m.p.: 125–127°C; IR (KBr, cm^{-1}) ν: 1624, 1595 (C=C), 1513, 1334 (–NO_2); ^{1}H NMR ($CDCl_3$, 400 MHz) δ: 7.96–7.93 (d, 1H, $J = 13.6$ Hz, NO_2CH–), 7.53–7.49 (d, 1H, $J = 13.6$ Hz, C=CH–), 7.44–7.42 (d, 2H, $J = 7.2$ Hz, *o*-ArC–H), 7.40–7.37 (t, 2H, $J = 7.2$ Hz, *m*-ArC–H), 7.34–7.33 (d, 1H, $J = 7.2$ Hz, *p*-ArC–H), 7.11–7.09 (dd, 1H, $J = 8.4$, 2.0 Hz, Ar–H), 7.03–7.02 (d, 1H, $J = 2.0$ Hz, Ar–H), 6.93–6.91 (d, 1H, $J = 8.4$ Hz, Ar–H), 5.22 (s, 2H, OCH_2–), 3.93 (s, 3H, OCH_3–); and MS (ESI) *m/z*: 285.3, found: 286.1 $[M+H]^+$.

*3-Methoxy-4-benzyloxyphenethylamine (**2**)*

A solution of compound **1** (9.03 g, 31.68 mmol) in tetrahydrofuran (160 mL) was added dropwise to a suspension of lithium aluminum hydride (3.37 g, 88.72 mmol) in ethyl ether (80 mL) and tetrahydrofuran (80 mL) at 0°C over a period of 1 h. The reaction mixture was heated to reflux at 60°C for 2 h and then cooled to room temperature. Then, water (6 mL) and tetrahydrofuran (12 mL) were added, followed by 10% sodium hydroxide solution (6 mL). The salts were removed by filtration, and the filtrate was dried over anhydrous sodium sulfate. The solvent was removed under reduced pressure, and the crude product was purified by column chromatography on silica gel eluted with 100:20:0.2 dichloromethane/ethanol/triethylamine to produce compound **2** (5.26 g, 65%) as a yellow oil with the following properties: IR (KBr, cm^{-1}) ν: 3361 (–NH_2); ^{1}H NMR ($CDCl_3$, 400 MHz) δ: 7.44–7.42 (d, 2H, $J = 7.2$ Hz, *o*-ArC–H), 7.37–7.34 (t, 2H, $J = 7.2$ Hz, *m*-ArC–H), 7.30–7.29 (d, 1H, $J = 7.2$ Hz, *p*-ArC–H), 6.83–6.81 (d, 1H, $J = 8.0$ Hz, Ar–H), 6.75–6.74 (d, 1H, $J = 2.0$ Hz, Ar–H), 6.68–6.66 (dd, 1H, $J = 8.0$, 2.0 Hz, Ar–H), 5.13 (s, 2H, OCH_2–), 3.88 (s, 3H, OCH_3–), 2.95–2.92 (t, 2H, $J = 6.8$ Hz, Ar–CH_2–), 2.69–2.66 (t, 2H, $J = 6.8$ Hz, NH_2–CH_2–); and MS (ESI) *m/z*: 257.3, found: 258.1 $[M+H]^+$.

*6-Methoxy-7-benzyloxy-3,4-dihydroisoquinoline (**3**)*

Compound **2** (4.33 g, 16.85 mmol) was dissolved in acetic acid (24 mL) and trifluoroacetic acid (6 mL), and hexamethylenetetramine

(4.72 g, 33.67 mmol) was then added and stirred at room temperature for 30 min. The reaction mixture was heated to reflux at 80°C for 2 h and then cooled to room temperature. The cooled solution was diluted with water (50 mL), basified with 20% sodium hydroxide solution (50 mL), and extracted with dichloromethane (3 × 100 mL). Organic extracts were combined and concentrated in a vacuum. The crude product was purified by column chromatography on silica gel eluted with 100:3 dichloromethane/ethanol to produce compound **3** (2.9 g, 65%) as a pale yellow oil with the following properties: ^{1}H NMR ($CDCl_3$, 400 MHz) δ: 8.15 (s, 1H, N–CH–), 7.46–7.44 (d, 2H, J = 7.2 Hz, *o*-ArC–H), 7.40–7.36 (t, 2H, J = 7.2 Hz, *m*-ArC–H), 7.33–7.32 (d, 1H, J = 7.2 Hz, *p*-ArC–H), 6.83 (s, 1H, ph, quinoline-H), 6.69 (s, 1H, ph, quinoline-H), 5.15 (s, 2H, OCH_2–), 3.92 (s, 3H, OCH_3–), 3.74–3.69 (m, 2H, NCH_2CH_2–), 2.69–2.65 (t, 2H, J = 7.8 Hz, N–CH_2–); and MS (ESI) *m*/*z*: 267.3, found: 268.1 $[M+H]^+$.

*3-Isobutyl-9-methoxy-10-benzyloxy-2,3,4,6,7,11b-hexahydro-1H-pyrido[2,1-a]isoquinoline-2-one (10-BnO-TBZ) (**4**)*

3-Dimethylaminomethyl-5-methyl-hexan-2-one (1.2 g, 6.55 mmol), compound **3** (1.45 g, 5.4 mmol), and TEBAC (0.38 g, 1.65 mmol) were dissolved in water (25 mL). The mixture was stirred and heated under reflux at 90°C for 4 h. The solvent was then removed under reduced pressure, and the crude product was purified by crystallization with ethanol, which yielded compound **4** (1.04 g, 49%) as a yellow crystal with the following properties: m.p.: 133–135°C; ^{1}H NMR ($CDCl_3$, 400 MHz) δ: 7.43–7.41 (d, 2H, J = 7.2 Hz, *o*-ArC–H), 7.37–7.34 (t, 2H, J = 7.2 Hz, *m*-ArC–H), 7.30–7.28 (d, 1H, J = 7.2 Hz, *p*-ArC–H), 6.64 (s, 1H, ph, quinolizine-H), 6.57 (s, 1H, ph, quinolizine-H), 5.09 (s, 2H, OCH_2–), 3.86 (s, 3H, OCH_3–), 3.45–3.42 (m, 1H, –CH–), 3.28–3.24 (dd, J = 6.4, 6.4 Hz, 1H, –CH–), 3.14–3.06 (m, 2H, –CH–), 2.77–2.65 (m, 3H, –CH–), 2.62–2.54 (m, 1H, –CH–), 2.46–2.40 (t, 1H, J = 12.4 Hz, –CH–), 2.35–2.29 (t, 1H, J = 11.8 Hz, –CH–), 1.82–1.75 (m, 1H, –CH–), 1.70–1.67 (m, 1H, –CH–), 1.05–0.98 (m, 1H, –$CH(CH_3)$), 0.92–0.89 (dd, 6H, J = 5.2, 5.2 Hz, –CH_3); and MS (ESI) *m*/*z*: 393.5, found: 394.2 $[M+H]^+$.

*3-Isobutyl-9-methoxy-10-benzyloxy-2,3,4,6,7,11b-hexahydro-1H-pyrido[2,1-a]isoquinoline-2-ol (10-BnO-DTBZ) (**5**)*

Compound **4** (1.0 g, 2.54 mmol) was dissolved in ethanol (60 mL), and sodium borohydride (0.97 g, 25.4 mmol) was then added and stirred at room temperature for 16 h. The mixture was diluted with water (50 mL) and dichloromethane (50 mL) and then extracted with dichloromethane (2 × 50 mL). Organic extracts were combined and concentrated in a vacuum. The crude product was purified by crystallization with methanol to produce compound **5** (0.67 g, 67%) as a white crystal with the following properties: m.p.: 178–180°C; ^{1}H NMR ($CDCl_3$, 400 MHz) δ: 7.44–7.42 (d, 2H, J = 7.2 Hz, *o*-ArC–H), 7.38–7.34 (t, 2H, J = 7.2 Hz, *m*-ArC–H), 7.31–7.29 (d, 1H, J = 7.2 Hz, *p*-ArC–H), 6.71 (s, 1H, ph, quinolizine-H), 6.60 (s, 1H, ph, quinolizine-H), 5.10 (s, 2H, OCH_2–), 3.85 (s, 3H, OCH_3–), 3.38–3.32 (m, 1H, –CH–), 3.13–2.93 (m, 4H, –CH–), 2.65–2.61 (m, 1H, –CH–), 2.47–2.40 (m, 1H, –CH–), 1.98–1.92 (t, 1H, J = 11.4 Hz, –CH–), 1.74–1.66 (m, 2H, –CH–), 1.58–1.36 (m, 3H, –CH–), 1.08–1.01 (m, 1H, –$CH(CH_3)$), 0.94–0.90 (dd, 6H, J = 6.4, 6.4 Hz, –CH_3); and MS (ESI) *m*/*z*: 395.5, found: 396.2 $[M+H]^+$.

*3-Isobutyl-9-methoxy-2,3,4,6,7,11b-hexahydro-1H-pyrido[2,1-a]isoquinoline-2,10-diol (10-O-desmethyl-DTBZ) (**6**)*

Compound **5** (0.33 g, 0.84 mmol) was dissolved in ethanol (50 mL), followed by the addition of 10% palladium on carbon (0.1 g) and the mixture was hydrogenated at room temperature for 16 h. The reaction mixture was filtered, and the filtrate was dried over anhydrous sodium sulfate. The solvent was removed under reduced pressure, and the crude product was purified by column chromatography on silica gel eluted with 100:4 dichloromethane/methanol to produce compound **6** (0.16 g, 63%) as a pink solid with the following properties: IR (KBr, cm^{-1}) ν: 3099 (–OH), 2949 (–CH_3); ^{1}H NMR ($CDCl_3$, 400 MHz) δ: 6.74 (s, 1H, ph, quinolizine-H), 6.56 (s, 1H, ph, quinolizine-H), 3.85 (s, 3H, OCH_3–), 3.41–3.34 (m, 1H, –CH–), 3.13–3.10 (m, 2H, –CH–), 3.06–2.99 (m, 2H, –CH–), 2.68–2.61 (m, 2H, –CH–), 2.56–2.43 (m, 2H, –CH–), 2.00–1.95 (t, 1H, J = 11.4 Hz, –CH–), 1.63–1.59 (m, 1H, –CH–), 1.52–1.46 (t, 2H, J = 11.8 Hz, –CH–), 1.08–1.01 (m, 1H, –$CH(CH_3)$), 0.95–0.91 (dd, 6H, J = 6.4, 6.4 Hz, –CH_3); and MS (ESI) *m*/*z*: 305.4, found: 306.1 $[M+H]^+$.

*3-Isobutyl-9-methoxy-10-[^{11}C]-methoxy -2,3,4,6,7,11b-hexahydro-1H-pyrido[2,1-a]isoquinoline-2-ol (10-^{11}C-DTBZ) (**7**)*

Precursor product **6** (1.0 mg) was dissolved in dimethyl sulfoxide (0.3 mL) with 3 N potassium hydroxide (4.0 μL). The ^{11}C-methyl iodide synthesized was transferred to the reaction vessel via a nitrogen stream. After reacting at room temperature for 3 min, the reaction mixture was transferred and loaded onto an alumina Sep-Pak cartridge (previously activated with 7 mL of ethyl ether with 1% ethanol). The Sep-Pak cartridge was washed with 1 mL of ethyl ether with 1% ethanol to remove the radioactive impurities and then eluted with 4 mL of ethyl ether with 1% ethanol. The solution was blown dry with N_2 for 2 min to yield 10-^{11}C-DTBZ. Product **7** was diluted with saline and stored for further use.

Quality control

The RCP of 10-^{11}C-DTBZ was determined by radio-HPLC using a Waters 600-type HPLC system with a Symmetry C_{18} reversed-phase column (5 μm, 4.6 mm × 150 mm, Waters). 10-^{11}C-DTBZ was isocratically eluted with acetonitrile and 0.05 M ammonium acetate (20:80 v/v, pH 4.0) at a flow rate of 0.8 mL/min and then identified by co-injection with the unlabeled reference compound DTBZ. DTBZ was monitored with a UV detector at 280 nm. The chemical purity of 10-^{11}C-DTBZ after purification was determined by HPLC with UV detection at 280 nm.

MicroPET imaging

Imaging was performed using a Siemens Inveon 5000 microPET system (Siemens, Germany). The microPET scanner had an effective axial field of view (FOV) of 12.7 cm. The resolution at the center of the FOV was 1.4 mm. Three normal rats and three 6-OHDA unilaterally lesioned rats were used for PET image acquisition. Rats were anesthetized with 1.5% isoflurane in oxygen, positioned on the bed of the microPET gantry, and fixed near the center of the scanner. Isoflurane anesthesia was continued throughout the study. Each rat was injected intravenously via the tail vein with an average of 29.4 MBq (0.8 mCi) of 10-^{11}C-DTBZ in saline. The scan duration was 60 min from the time of injection.

Scans were obtained in the frame sequence 6×10 s, 6×60 s, 4×120 s, and 9×300 s. The data were histogrammed into 25 consecutive frames, and the images were reconstructed using a three-dimensional ordered subsets expectation maximum (OSEM) algorithm. Normalization and scatter correction were performed during the reconstructions. Images were analyzed with ASIProVM (Concorde Microsystems, USA). Frames from 8 to 60 min were summed to manually draw regions of interest (ROIs). ROIs were drawn manually from two brain regions (striatum and cerebellum) on coronal slices guided by a mouse brain stereotaxic atlas, and time–activity curves (TACS) for the ROIs were obtained. Radioactivity concentrations (nCi/cc) were normalized to the injected dose of the radiotracer.

The authors are very grateful to the National Natural Science Foundation of China (30970844), Natural Science Foundation of Jiangsu Province (BK2010155), Outstanding Professionals Foundation of Jiangsu Health Bureau (RC2011096) and Public Service Platform for Science and Technology Infrastructure Construction Project of Jiangsu Province (BM2012066) for their financial support.

The authors have declared no conflict of interest.

References

[1] D. C. German, P. K. Sonsalla, *Adv. Behav. Biol.* **2003**, *54*, 131–137.

[2] N. I. Bohnen, R. A. Koeppe, P. Meyer, E. Ficaro, K. Wernette, M. R. Kilbourn, D. E. Kuhl, K. A. Frey, R. L. Albin, *Neurology* **2000**, *54*, 1753–1759.

[3] S. Gilman, R. A. Koeppe, R. Little, H. An, L. Junck, B. Giordani, C. Persad, M. Heumann, K. Wernette, *Ann. Neurol.* **2004**, *55*, 774–780.

[4] J. K. Zubieta, S. F. Taylor, P. Huguelet, R. A. Koeppe, M. R. Kilbourn, K. A. Frey, *Biol. Psychiatry* **2001**, *49*, 110–116.

[5] J. N. DaSilva, J. E. Carey, P. S. Sherman, T. J. Pisani, M. R. Kilbourn, *Nucl. Med. Biol.* **1994**, *21*, 151–156.

[6] J. P. Henry, B. Gasnier, M. F. Isambert, F. Darchen, D. Scherman, *Adv. Biosci.* **1991**, *82*, 147–150.

[7] D. K. Miller, P. A. Crooks, G. Zheng, V. P. Grinevich, S. Norrholm, L. P. Dwoskin, *J. Pharmacol. Exp. Ther.* **2004**, *310*, 1035–1045.

[8] R. P. Perera, D. S. Wimalasena, K. Wimalasena, *J. Med. Chem.* **2003**, *46*, 2599–2605.

[9] M. R. Kilbourn, J. N. DaSilva, K. A. Frey, R. A. Koeppe, D. E. Kuhl, *J. Neurochem.* **1993**, *60*, 2315–2318.

[10] R. A. Koeppe, K. A. Frey, A. Kume, R. Albin, M. R. Kilbourn, D. E. Kuhl, *J. Cereb. Blood Flow Metab.* **1997**, *17*, 919–931.

[11] M. R. Kilbourn, P. S. Sherman, L. C. Abbott, *Nucl. Med. Biol.* **1995**, *22*, 565–567.

[12] L. Zhu, Y. J. Liu, K. Plössl, B. Lieberman, J. Liu, H. F. Kung, *Nucl. Med. Biol.* **2010**, *37*, 133–141.

[13] D. Scherman, R. Raisman, A. Ploska, Y. Agid, *J. Neurochem.* **1988**, *50*, 1131–1136.

[14] M. R. Kilbourn, P. S. Sherman, *Eur. J. Pharmacol.* **1997**, *331*, 161–168.

[15] M. R. Kilbourn, E. R. Butch, T. Desmond, P. Sherman, P. E. Harris, K. A. Frey, *Nucl. Med. Biol.* **2010**, *37*, 3–8.

[16] R. A. Koeppe, S. Gilman, L. Junck, K. Wernette, K. A. Frey, *Alzheimers Dement.* **2008**, *4*, S67–S76.

[17] X. M. Li, Z. P. Chen, C. Y. Liu, J. Tang, *J. Chem. Ind. Eng.* **2012**, *63*, 567–571.

[18] G. Quincoces, M. Collantes, R. Catalan, M. Ecay, E. Prieto, E. Martino, F. J. Blesa, L. Álvarez-Erviti, P. Areses, J. Arbizu, J. A. Obeso, J. M. Martí-Climent, J. A. Richter, I. Peñuelas, *Rev. Esp. Med. Nucl.* **2008**, *27*, 13–21.

[19] J. N. DaSilva, M. R. Kilbourn, E. F. Domino, *Synapse* **1993**, *14*, 128–131.

[20] T. M. Vanden Borght, M. R. Kilbourn, R. A. Koeppe, J. N. DaSilva, J. E. Carey, D. E. Kuhl, K. A. Frey, *J. Nucl. Med.* **1995**, *36*, 2252–2260.

[21] G. L. Chan, J. E. Holden, A. J. Stoessl, A. Samii, D. J. Doudet, T. Dobko, K. S. Morrison, M. Adam, M. Schulzer, D. B. Calne, T. J. Ruth, *J. Nucl. Med.* **1999**, *40*, 283–289.

[22] J. M. Zhang, X. J. Zhang, Y. G. Li, J. H. Tian, *Molecules* **2012**, *17*, 6697–6704.

[23] R. Goswami, D. E. Ponde, M. P. Kung, C. Hou, M. R. Kilbourn, H. F. Kung, *Nucl. Med. Biol.* **2006**, *33*, 685–694.

[24] M. R. Kilbourn, B. Hockley, L. C. Lee, C. Hou, R. Goswami, D. E. Ponde, M. P. Kung, H. F. Kung, *Nucl. Med. Biol.* **2007**, *34*, 233–237.

[25] J. N. DaSilva, M. R. Kilbourn, *Life Sci.* **1992**, *51*, 593–600.

[26] Z. P. Chen, C. Y. Liu, X. M. Li, J. Tang, C. Tan, H. B. Huang, H. X. Yu, S. N. Luo, *Nucl. Sci. Technol.* **2012**, *23*, 40–46.

[27] M. Collantes, I. Penuelas, L. Alvarez-Erviti, J. Blesa, J. M. Marti-Climent, G. Quincoces, M. Delgado, M. Ecay, A. Martinez, J. Arbizu, M. C. Rodriguez-Oroz, J. Obeso, J. A. Richter, *Rev. Esp. Med. Nucl.* **2008**, *27*, 103–111.

[28] M. R. Kilbourn, L. C. Lee, T. M. Vanden Borght, D. M. Jewett, K. A. Frey, *Eur. J. Pharmacol.* **1995**, *278*, 249–252.

[29] S. P. Wang, Z. P. Chen, X. M. Li, J. Tang, C. Y. Liu, M. F. Zou, D. H. Pan, C. X. Lu, Y. P. Xu, X. J. Xu, X. Q. Zhou, J. Jin, *Nucl. Sci. Technol.* **2009**, *20*, 11–16.

